AD-A125 663 DETERMINING SOURCE PARAMETERS OF MODERATE-SIZE EARTHQUAKES FROM REGIONAL..(U) CALIFORNIA INST OF TECH PASADENA SEISMOLOGICAL LAB T C WALLACE ET AL. 1/1

UNCLASSIFIED 29 OCT 81 AFOSR-TR-83-0097 F49620-77-C-0022 F/G 8/11 NL

END
DATE FILMED
4 83
DTIC

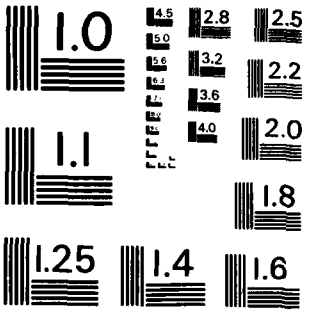

MICROCOPY RESOLUTION TEST CHART
NATIONAL BUREAU OF STANDARDS - 1963 - A

UNCLASSIFIED
SECURITY CLASSIFICATION OF THIS PAGE (When Data Entered)

FEB 1 1983

(2)

REPORT DOCUMENTATION PAGE	READ INSTRUCTIONS BEFORE COMPLETING FORM
1. REPORT NUMBER: AFOSR-TR- 83-0097	2. GOVT ACCESSION NO. / 3. RECIPIENT'S CATALOG NUMBER
4. TITLE (and Subtitle): Determining Source Parameters of Moderate-Size Earthquakes from Regional Waveforms	5. TYPE OF REPORT & PERIOD COVERED: REPRINT
	6. PERFORMING ORG. REPORT NUMBER
7. AUTHOR(s): Terry C. Wallace and Donald V. Helmberger	8. CONTRACT OR GRANT NUMBER(s): F49620-77-C-0022
9. PERFORMING ORGANIZATION NAME AND ADDRESS: California Institute of Technology, Seismological Laboratory 252-21, Pasadena, CA 91125	10. PROGRAM ELEMENT, PROJECT, TASK AREA & WORK UNIT NUMBERS: 3291-40 PE:62714E PC:1A10
11. CONTROLLING OFFICE NAME AND ADDRESS: Advanced Research Projects Agency/NMR, 1400 Wilson Boulevard, Arlington, VA 22209	12. REPORT DATE: 1982 / 13. NUMBER OF PAGES: 12
14. MONITORING AGENCY NAME & ADDRESS(if different from Controlling Office): Air Force Office of Scientific Research, Bolling Air Force Base, DC 20332, Attention: NP	15. SECURITY CLASS. (of this report): UNCLASSIFIED / 15a. DECLASSIFICATION/DOWNGRADING SCHEDULE

16. DISTRIBUTION STATEMENT (of this Report)
Approved for public release; distribution unlimited.

17. DISTRIBUTION STATEMENT (of the abstract entered in Block 20, if different from Report)
Physics of the Earth and Planetary Interiors, v. 30, pp. 185-196., 1982

18. SUPPLEMENTARY NOTES

DTIC ELECTE S MAR 15 1983 D B

19. KEY WORDS (Continue on reverse side if necessary and identify by block number)
Source parameters/Regional waveforms

20. ABSTRACT (Continue on reverse side if necessary and identify by block number)

Waveform modeling of the teleseismic long-period body-wave phases of shallow earthquakes has proven quite effective in determining source parameters for events of magnitude larger than six. Unfortunately, these teleseismic phases become too weak for smaller events, and regional data must be used which are generally much more complicated. This is because the crust-mantle system acts as a leaky waveguide and a large number of rays are required to model the observations. In this report we review a procedure for the

DD FORM 1 JAN 73 1473

83 03 14 139

UNCLASSIFIED
SECURITY CLASSIFICATION OF THIS PAGE (When Data Entered)

AD A125013

DTIC FILE COPY

20. systematic determination of source parameters from regional body waves. A least-squares inversion technique is used which is based on a cross-correlation of the data and a synthetic seismogram. The synthetic waveforms are a linear combination of those for the three fundamental types of fault. A set of profiles of the synthetic waveforms is presented. Although the synthetic waveforms are generated for a model developed for the western United States, this model seems to be adequate for most continental regions. The inversion is parameterized in terms of fault strike, dip and rake; these parameters are relatively insensitive to small changes in crustal structure. Several examples are presented.

Physics of the Earth and Planetary Interiors, 30 (1982) 185–196
Elsevier Scientific Publishing Company, Amsterdam – Printed in The Netherlands

Determining source parameters of moderate-size earthquakes from regional waveforms *

Terry C. Wallace and Don V. Helmberger

Seismological Laboratory, California Institute of Technology, Pasadena, CA 91125 (U.S.A.)

(Received October 29, 1981; revision accepted February 20, 1982)

Wallace, T.C. and Helmberger, D.V., 1982. Determining source parameters of moderate-size earthquakes from regional waveforms. Phys. Earth Planet. Inter., 30: 185–196.

Waveform modeling of the teleseismic long-period body-wave phases of shallow earthquakes has proven quite effective in determining source parameters for events of magnitude larger than six. Unfortunately, these teleseismic phases become too weak for smaller events, and regional data must be used which are generally much more complicated. This is because the crust–mantle system acts as a leaky waveguide and a large number of rays are required to model the observations. In this report we review a procedure for the systematic determination of source parameters from regional body waves. A least-squares inversion technique is used which is based on a cross-correlation of the data and a synthetic seismogram. The synthetic waveforms are a linear combination of those for the three fundamental types of fault. A set of profiles of the synthetic waveforms is presented. Although the synthetic waveforms are generated for a model developed for the western United States, this model seems to be adequate for most continental regions. The inversion is parameterized in terms of fault strike, dip and rake; these parameters are relatively insensitive to small changes in crustal structure. Several examples are presented.

1. Introduction

A considerable amount of effort has been expended to determine the source parameters of moderate-size earthquakes, although such determinations can be beset with difficulties. Ideally, a large amount of information can be derived from the modeling of long-period body waves (see Helmberger, 1974; Langston and Helmberger, 1975). Unfortunately, if an earthquake is too small to be well recorded teleseismically, which is the case for many events in the magnitude range between 5 and 6, the fault-plane orientation must be constrained by local short-period data and the seismic moment usually cannot be determined unambiguously. The World-Wide Standard Seismograph Network (WWSSN) supplemented by other long-period stations and arrays provides sufficiently dense coverage, in that most moderate-size earthquakes occurring in continental regions will produce some on-scale records of long-period body waves at regional distances. In the regional distance range (1–12°), the waveguide properties of the crust produce complicated body-wave signals; however, in most cases the long-period waveform is quite distinctive and sufficiently insensitive to details of crustal structure to allow the separation of the source and structural information.

In this paper we review a procedure for extracting the source parameters of moderate-size earthquakes from data for long-period regional phases. The technique involves an iterative inversion pro-

* Contribution No. 3706, Division of Geological and Planetary Sciences, California Institute of Technology, Pasadena, CA 91125, U.S.A.

0031-9201/82/0000–0000/$02.75

cess which minimizes the difference between a synthetic seismogram and the observation. The synthetic waveforms are constructed using Green's functions computed for a single, very simple structure. These Green's functions appear to be an adequate model for most continental regions, thus allowing a quick and approximate determination of fault parameters. The inversion is parameterized in terms of strike, dip and rake. The number of inversion parameters has been minimized so that inadequacies in the Green's functions are not overemphasized. Obviously, the structural model is more appropriate for certain regions than for others, so the inversion parameters chosen are those which are most robust. The main advantage of the technique is that it requires only a small data set. The general usefulness of this technique is illustrated by inverting regional data for earthquakes occurring in the United States, northern Canada and southern Europe.

2. The Green's functions

The techniques for constructing the Green's functions have been discussed in detail elsewhere (Helmberger and Engen, 1980; Wallace et al., 1981). What is discussed here is some simplifying approximations and their applicability. The waveform of interest is that part of a regional seismogram which arrives before the S-wave. This waveform is referred to as P_{nl}. It is simplest to discuss P_{nl} in terms of rays which are in a waveguide. The first part of P_{nl} is dominated by P waves (Pn) and, moving back into the record, the waveform contains progressively more SV (PL) contributions. The SV energy corresponds to rays which are reflected within the crust and undergo subsequent mode changes at the free surface and the Moho. The interference of all the rays gives rise to the waveform; parameters such as the crustal thickness or the velocity contrast between the crust and the Moho control the waveform dispersion. Figure 1 shows some typical P_{nl} waveforms.

The Green's functions are constructed by summing generalized rays for a point shear dislocation. As an example, consider the following equation for the vertical displacement, in cylindrical

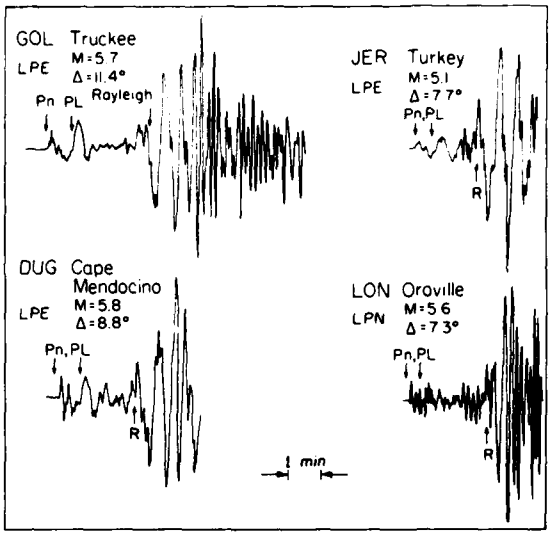

Fig. 1. The horizontal component of motion for four moderate-size earthquakes. The magnitude and distance to the recording station are given for each. Clockwise from the upper left: (1) September 12, 1966, Truckee, CA, strike-slip event; (2) June 13, 1965, southwest Turkey, normal event; (3) August 1, 1975, Oroville, CA, normal event; and (4) December 10, 1967, off the coast near Cape Mendocino, CA, strike-slip event.

coordinates

$$w(r,z,\theta,t) = (M_0/4\pi\rho)\left(\dot{D}(t) * \sum_{i=1}^{3} W_i(t)A_i\right) \tag{1}$$

where $\dot{D}(t)$ is the far-field time history, ρ the source region density, and M_0 the seismic moment. The summation process adds the contributions of the three fundamental types of fault; W_i are the Green's functions for vertical strike-slip, vertical dip-slip and 45° dip-slip step dislocations, respectively. A_i are coefficients determined by the source orientation and are given by

$$\begin{aligned} A_1(\theta,\lambda,\delta) &= \sin 2\theta \cos\lambda \sin\delta \\ &\quad + (1/2)\cos 2\theta \sin\lambda \sin 2\delta \\ A_2(\theta,\lambda,\delta) &= \cos\theta \cos\lambda \cos\delta - \sin\theta \sin\lambda \cos 2\delta \\ A_3(\theta,\lambda,\delta) &= (1/2)\sin\lambda \sin 2\theta \end{aligned} \tag{2}$$

where θ is the receiver azimuth from the end of the fault plane, λ is the rake angle, and δ is the dip angle. The total displacement is then the sum of the displacements from each ray. The number of rays which are used is determined by the structure and the pass band of the observation. In our previous work we have shown that a single layer, corresponding to the crust, over a half-space mantle is a sufficient structural model for regional long-period records to allow the extraction of the source parameters of moderate-size earthquakes.

As an example, Fig. 2 shows a comparison of the synthetic waveforms and the records of the 1966 Truckee, CA earthquake (which will be discussed in more detail). The synthetic waveforms were constructed from Green's functions computed for the crustal model in Table I, and the fault orientation was determined by inversion of the regional data. In this case the source time function and moment were determined by other methods, so that the synthetic amplitudes can be viewed as predictions. The numbers on the traces are maximum peak-to-peak amplitudes. The only noticeable difference between the data and the synthetic waveforms concerns the high-frequency content, which could be caused by several factors: (1) the effects of attenuation within the crust have not been added to the synthetic waveforms, and (2) the very sharp boundaries in our model are efficient in trapping short-period energy. Overall,

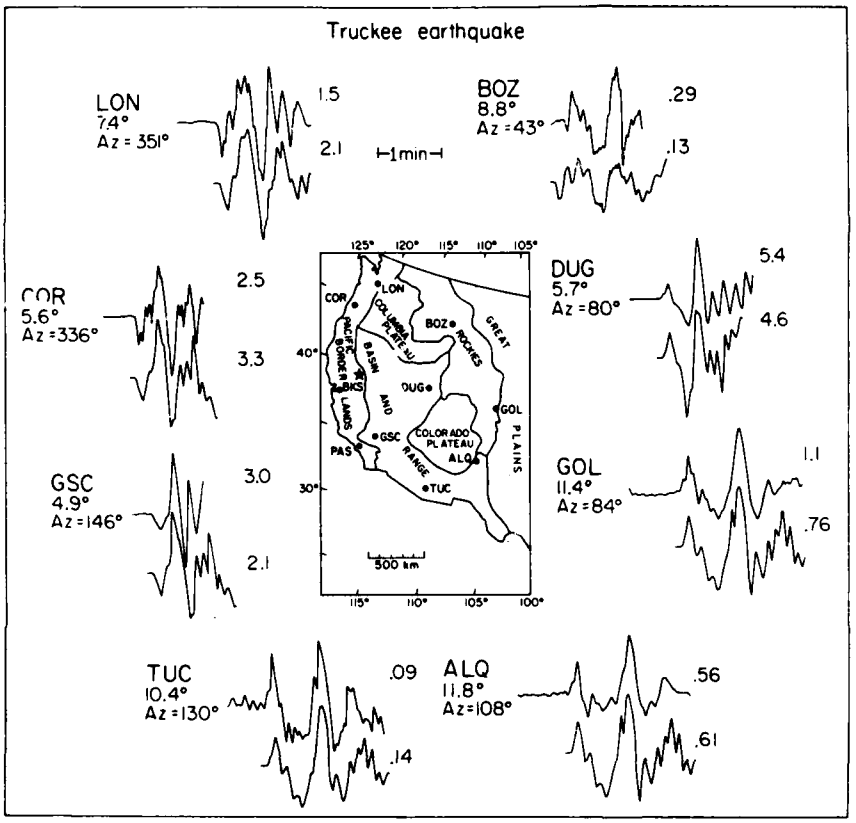

Fig. 2. Vertical P_{nl} waveforms from the Truckee earthquake. The star denotes the epicenter. The data are the top trace at each station, the trace below is the synthetic fit. The strike–slip mechanism has two nodal planes which project through the stations TUC and BOZ. To the right of each trace is the observed or predicted amplitude (on the basis of a moment of 0.8×10^{25} dyne cm) in 10^{-3} cm.

TABLE I

Crustal model

v_p (km s^{-1})	v_s (km s^{-1})	Density (g cm^{-3})	Layer thickness (km)
6.2	3.5	2.7	32
8.2	4.5	3.4	

the fit of the synthetic waveforms to the data justifies the use of the simple model, and the high-frequency content of the synthetic waveforms does not affect our ability to determine the source parameters.

The only expensive or complicated part of this modeling process is the actual generation of the Green's functions. For this reason, Figs. 3 and 4 are presented, which give profiles of the vertical and radial responses for the three fundamental faults. Most earthquakes which produce an on-scale P_{nl} at long-period WWSSN stations have similar time functions (which is simply a reflection of event size). In Figs. 3 and 4 a trapezoid with a 1 s rise, a 1 s top and a 1 s fall is used for the

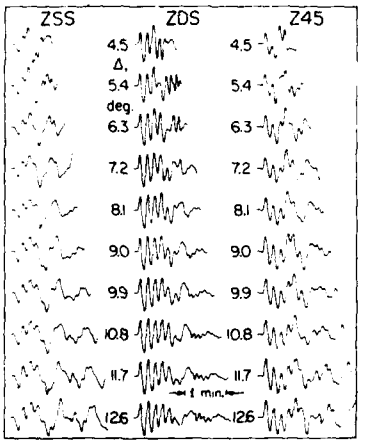

Fig. 3. Theoretical displacement profiles for the vertical component. The Green's functions were computed from the model presented in Table I and have been convolved with a source time function represented by a trapezoid ($t_1 = 1, t_2 = 1, t_3 = 1$), a triangular filter (2 s rise and fall), and the response function for a WWSSN long-period instrument.

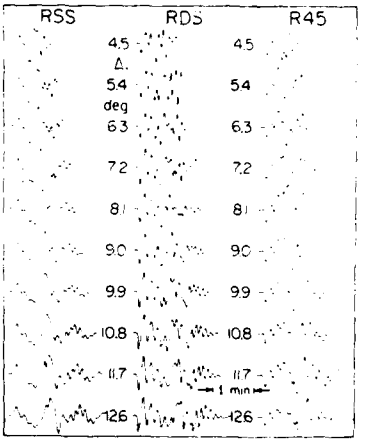

Fig. 4. Theoretical displacement profiles for the radial component. The Green's functions are computed every 100 km. They have been convolved with the time function, instrument response and filter described in Fig. 3.

far-field time history. The displacements have also been convolved with the response function for a 15–100 instrument. Because of the differences in high-frequency content between the data and the synthetic waveforms, the displacement responses have also been filtered. The filter has an impulse response represented by a triangle which has a 2 s rise and fall. When comparing these displacements with the data, the observations should be similarly filtered. Once the response for the three fundamental faults is known any seismogram can be constructed by a linear combination of them.

The displacements in Figs. 3 and 4 were computed for a source depth of 8 km. Varying the source depth between 5 and 15 km has only a small effect on the waveform. This is easily understood by considering that to first order, a change in source depth affects only the travel time of the first segment of any ray. Figure 5 shows a comparison of the synthetic waveforms at 1000 km for three different source depths. After doubling the source depth (from 8 to 16 km) the essential character of the waveform is still preserved and the source information is retrievable. In contrast, a similar change in crustal thickness would affect the travel time of each leg of a given ray, hence significantly changing the waveform dispersion

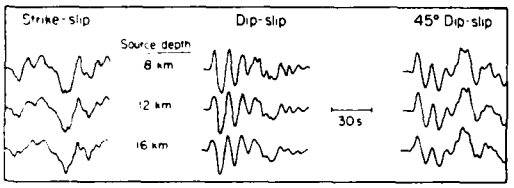

Fig. 5. P_{nl} waveforms at 1000 km for three different source depths.

(Wallace and Helmberger, 1980). The insensitivity of the displacements to source depth allows the responses in Figs. 3 and 4 to be used, at least in a qualitative fashion, to determine the source parameters of most crustal earthquakes.

The only other major question concerning the applicability of the displacements presented relates to the structure used in their calculation. Experience indicates that the simplistic model adopted is justified. The model in Table I is an average developed for the western United States, although it appears to be sufficient for most continental regions in the world. The waveform dispersion is dependent on crustal thickness and on the contrast between the upper-mantle P velocity and the mean crustal P velocity, so obviously for regions having anomalous crustal structure, such as the Tibetan Plateau, the responses in Figs. 3 and 4 would be inadequate. Also, the use of the half-space to approximate the upper mantle must cease to be valid at some point; at some distance a significant amount of energy will be present in the form of diving rays which have turned in the mantle. For most continental regions this distance appears to be $\sim 12°$. If diving rays are present, the ratio of the Pn to PL amplitudes should differ from the synthetic value (Wallace and Helmberger, 1981). Also, the predicted amplitude should begin to diverge from that observed, owing to attenuation in the upper mantle. Figure 6 shows a profile of the Truckee earthquake records; the amplitudes have been corrected for the azimuthal radiation pattern and the polarities have been adjusted to show a smooth dispersion pattern. To the right is a profile of displacements for a strike-slip earthquake (such a profile can be constructed from Fig. 3). Note that there does not appear to be a

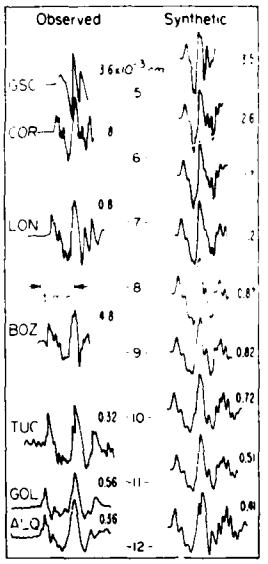

Fig. 6. Truckee earthquake waveforms corrected for horizontal radiation pattern and plotted as a function of distance. The maximum amplitude is shown to the right of each trace. Note that the stations BOZ and TUC are very close to nodes.

systematic break-down in waveform shape or amplitude over the distance range 4–12°. Also note that the stations BOZ and TUC are nearly nodal, and thus their recordings of amplitude are not particularly reliable.

3. Inversion technique

The ability to determine the source parameters of an earthquake by comparing an observed with a predicted waveform depends on the assessment of the quality of fit. In a previous paper (Wallace et al., 1981) we presented a least-squares waveform-inversion technique which makes use of an error function determined by the cross-correlation of a long-period seismogram and a synthetic waveform:

$$e = 1 - \int fg \Big/ \left(\int f^2\right)^{1/2} \left(\int g^2\right)^{1/2} \qquad (3)$$

where f is the observed record, g is the synthetic waveform, and the integral is a zero-lag cross-correlation. The limits of integration are the time

length of the window in which the waveforms are correlated. The denominator serves to normalize both the data and the synthetic waveform. This normalization process renders the error function insensitive to the absolute amplitudes. To minimize the error, which corresponds to maximizing the correlation, f and g are allowed to optimally align themselves with regard to waveform; f and g are aligned a priori in time by matching first breaks and ignoring absolute travel time. The error function can be rewritten by considering that the synthetic seismogram can be constructed using waveforms for the three fundamental faults. In this case there is a summation of the cross-correlations between the observed and each of the fundamental faults. For a given range, the cross-correlations are constant and errors can be minimized by varying the A_i's in eq. (2). In other words, once the cross-correlations are computed the source orientation is determined iteratively and only the constants have to be recalculated. For a detailed discussion of the inversion technique see Wallace et al. (1981).

Once the source orientation is fixed, the moment of an earthquake can be determined by comparing the amplitudes of the synthetic waveform and the observations. Adopting the units of Helmberger and Malone (1975), and expressing the range in km, time in s, density in g cm^{-3}, velocity in km s^{-1}, the moment in dyne cm, and displacement in cm, yields

$$M_0 = 4\pi\rho \times 10^{20}\left(\frac{\text{data amplitude}}{\text{synthetic amplitude}}\right) \qquad (4)$$

A moment can be determined by comparing the maximum peak-to-peak amplitudes for any time window used for the correlation. It has been found that a moment should be determined for a few peaks at a given station. The ratio of the moment at each station to the mean is a measure of the amplitude stability. In general, the moments determined from P_{nl} are in very good agreement with those determined teleseismically, using an assumption of $t^* = 1$ s.

4. Examples

We have inverted the P_{nl} waveforms from five earthquakes to demonstrate the utility of the technique. Three of the earthquakes occurred in the western United States. Two other earthquakes, one in Baffin Bay in the Artic and the other in Turkey, have been included to demonstrate that the Green's functions are not unique to the United States. Both dip-slip and strike-slip mechanisms are represented in the suite of examples.

4.1. Truckee, CA (12/9/67)

The Truckee earthquake was a strike-slip event at 10 km depth which produced excellent regional records but very few teleseismic body-wave records, as is typical of moderate-size strike-slip events. The Truckee earthquake ($m_b = 5.7$) has been studied by numerous authors (Ryall et al., 1968; Tsai and Aki, 1970; Burdick, 1977), making it a good test case. Tsai and Aki (1970), from first-motion studies and modeling of the surface waves, determined this event to be pure strike-slip on a fault plane striking N44°E and dipping 80°SE. The surface wave moment was determined to be 0.83×10^{25} dyne cm. Figure 2 shows the locations of the epicenter and the recording stations, and the filtered data for Truckee. Also shown are the synthetic waveforms determined from the inversion results. Note that the stations BOZ and TUC are very nearly nodal. The inversion yields a mechanism which is very similar to Tsai and Aki's (1970); a strike of N43°E, a dip of 76°SE, and a rake of $-11°$. The only significant difference is the slight dip-slip component in our solution, which is also acceptable on the basis of the first-motion data. The moment determined from the P_{nl} waveforms is 0.87×10^{25} dyne cm, which is in excellent agreement with the result obtained by Tsai and Aki (1970).

4.2. El Golfo, Mexico (7/8/66)

The El Golfo earthquake ($m_b = 6.3$, $M_s = 6.3$) was a strike-slip event which occurred near the mouth of the Colorado River at the northern end of the Gulf of California. Ebel et al. (1978) de-

termined the fault plane to be striking E140°S, dipping 85° to the southwest, and with a rake of 183°, and determined the depth of the event to be 10 km. Using teleseismic long-period P waves they determined a moment of 5.0×10^{25} dyne cm.

El Golfo is about the maximum-size event which can be used in the inversion technique. The P_{nl} records are barely on-scale at the stations used. Figure 7 shows the locations of the epicenter and the recording stations, and the waveforms. In this case the time function is a triangle with a 2 s rise and fall; the long-period impulse is a reflection of the event size. The long-period time function allows the use of a filter to be dispensed with. In Fig. 7, shown below the observed waveforms are the synthetic waveforms for the inversion solution, namely, for a strike of E137°S, a dip of 81°, and a rake of 175°. The inversion solution is in good agreement with the results of Ebel et al. (1978). The moment determined from the P_{nl} waveforms is 4.6×10^{25} dyne cm.

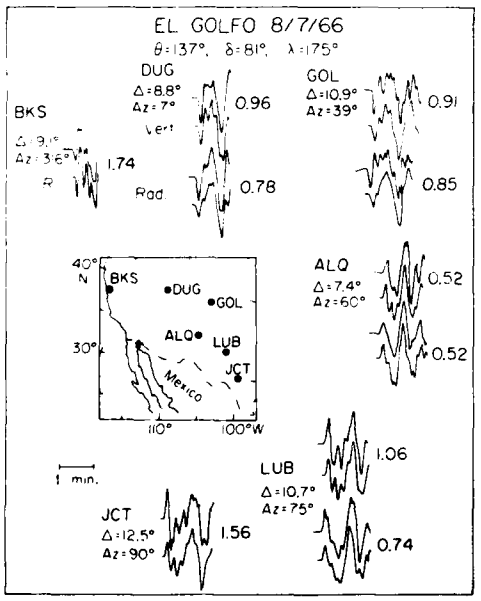

Fig. 7. Data and synthetic waveforms for the El Golfo earthquake. The map gives the location of the event (star) and the recording stations. Along each trace is the ratio of the station moment to the average moment.

4.3. *Oroville, CA (1/8/75)*

The Oroville earthquake ($M = 5.6$) was a normal faulting event and is interesting because the surface-wave (Hart et al., 1977) and body-wave (Langston and Butler, 1976) analyses yield substantially different moments. Langston and Butler (1976) determined the strike to be 180°, with a dip of 65° and a rake of −70°. Their moment determination is 5.7×10^{24} dyne cm. Hart et al. (1977) suggested that the surface waves are consistent with this body-wave mechanism but that the moment is larger by a factor of 3 (1.9×10^{25} dyne cm). Figure 8 shows the locations of the event, of the stations used in the inversion analysis, and the filtered data and synthetic waveforms. The inversion solution has shifted the mechanism to a strike of 204°, dipping 66° with a rake of −85°. This new solution violates only a few first motions, but the aftershock trend tends to support the 180° strike. The moment determined from P_{nl} data is 6.9×10^{24} dyne cm.

4.4. *Baffin Bay, Canada (4/9/63)*

The Baffin Bay earthquake ($M = 5.9$) was a normal event associated with a continental margin area. The travel path to each of the stations used in the inversion includes portions of crustal and oceanic regions, which makes it an ideal event to test the applicability of the Green's functions. Liu and Kanamori (1980) modeled the body waves and determined a fault-plane solution with a strike of 98°, a dip of 66°N, and a rake of −103°. The location of the event, and the filtered data and synthetic waveforms are shown in Fig. 9. The inversion solution has a mechanism striking 74°, dipping 66°, and with a rake of −100°. Again the only parameter which is appreciably different from the results of teleseismic analysis is the strike. In any case the inversion solution is acceptable, and the difference of 20° in strike can be considered as the resolution for dip–slip events.

4.5. *Turkey (13/6/65)*

The Turkish event ($M = 5.1$) was a shallow, normal event which occurred in southwest Turkey

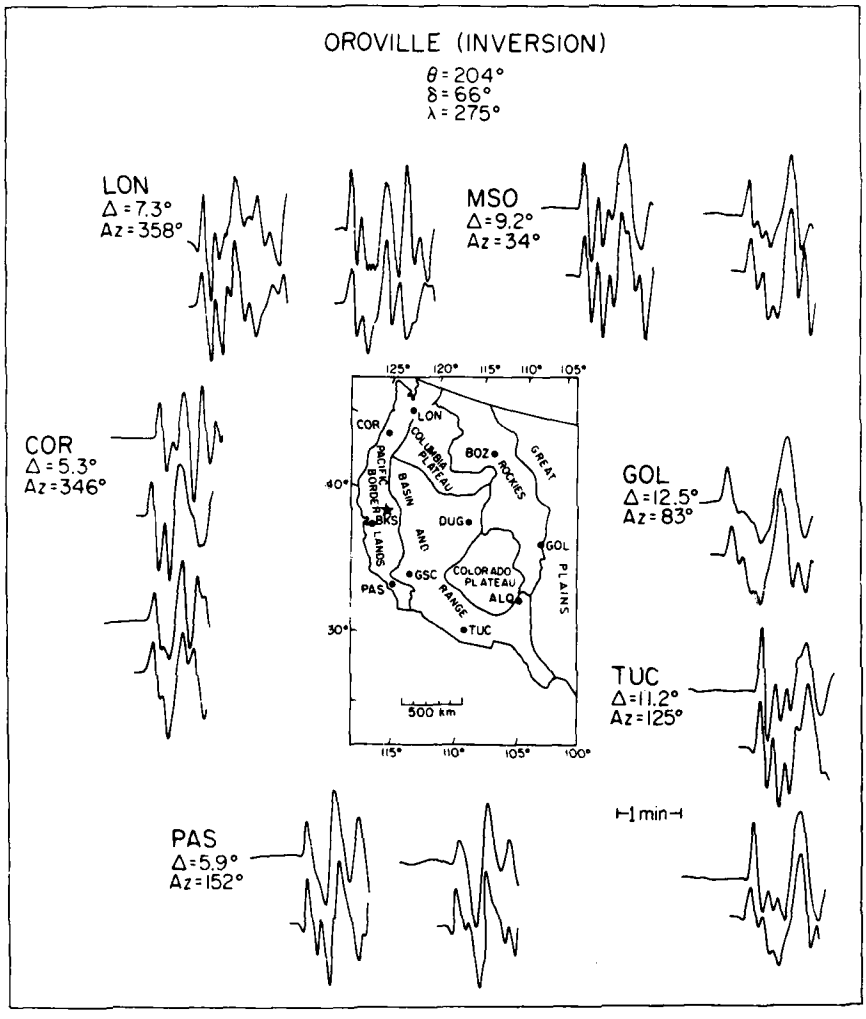

Fig. 8. Filtered data and synthetic waveforms for the Oroville earthquake. At all the stations except GOL both the vertical (the first trace pair) and radial components are shown.

in a region of north–south extension. McKenzie (1972) used first-motion data to determine a pure normal mechanism with a strike of 101° and dipping 70° to the south, although it is not well constrained. There were three WWSSN stations at regional distances which could be used in the inversion process. Figure 10 shows the locations of the event and the recording stations. The filtered data and the fit of the synthetic waveforms are also shown. The inversion solution (strike 131°, dip 68°, rake −88°) is consistent with the first-motion data, although it differs in strike from McKenzie's solution. Again the three-station solution is quite acceptable, considering the quality of the first-motion data.

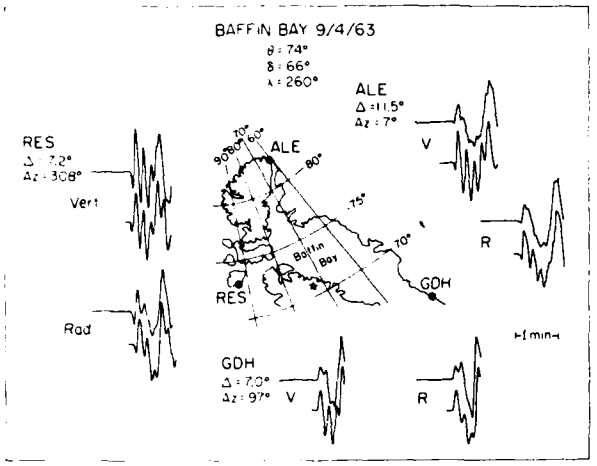

Fig. 9. Location of the Baffin Bay earthquake (star) and the recording stations. Filtered data and synthetic waveforms for both the vertical and radial components are shown.

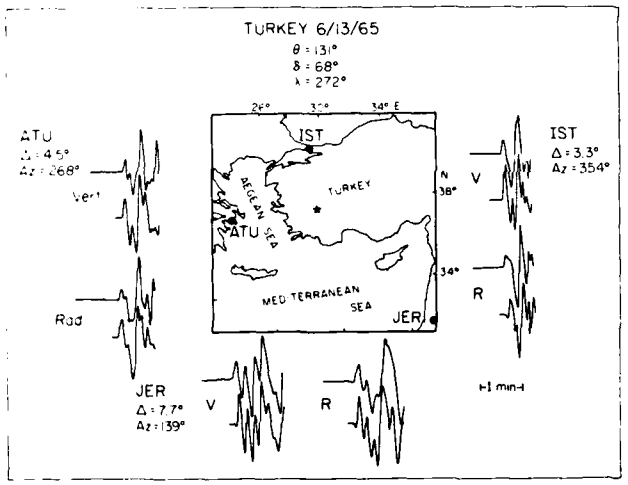

Fig. 10. Location of the Turkey earthquake (star) and the recording stations. Filtered data and synthetic waveforms for both the vertical and radial components are shown.

5. Discussion

Determining the fault-plane orientation of moderate-size earthquakes is often a frustrating experience, owing to the paucity of high-quality data. Earthquakes in the magnitude range 5–6 are quite important and are often the only "measurable" expression of the present tectonic environment. All of the available data must be used to extract the source parameters of these moderate-size events, and the modeling of P_{nl} waveforms can provide a valuable constraint in this process. Every situation will probably be unique and it is difficult to predict which data set will be the most defini-

tive. Nevertheless, it appears worthwhile to consider the P_{nl} inversion separately and its resolvability dependence on source orientation.

The inversion process discussed requires only a small data set. With ideal azimuthal separation, a data set comprising just three stations (vertical and radial components) can yield good solutions (it is possible to construct a case where the inversion is unstable, but in practice this has never happened). In almost all cases four recording stations are sufficient. P_{nl} should be polarized in the vertical and radial planes. Rotation of the horizontal components for a number of events indicates that there is very little energy on the tangential component, implying little contamination from such effects as multipathing. Therefore, it is usually sufficient to take the largest of the horizontal components to be the radial waveform in the inversion. The resolving ability of the inversion (or conversely, the error) depends on the type of earthquake. The experience gained by considering the examples presented in the last Section indicates that the mechanisms of strike–slip earthquakes can be determined quite well using data from relatively few stations. The strike is usually determined to within 5° of that determined by other methods. The rake is the least resolvable parameter for strike–slip events and can vary by up to 15° from that determined by first-motion studies. The mechanisms of dip–slip earthquakes are more difficult to determine. Although the dip and rake are usually determined in good agreement with other studies, the strike may vary by up to 20°. This feature is illustrated by considering a 45° dipping normal fault. In this case, most regional stations lie within the compressional region of the focal sphere and any given azimuth will produce remarkably similar waveforms. Fortunately, dip–slip events have rather strong teleseismic P waves, but again the waveforms are all the same, with little dependence on azimuth. In this case the stations lie in the center of the focal sphere and are all dilatational. As an example consider Fig. 11, which displays the focal sphere and the teleseismic waveforms for the Oroville earthquake. Note that the P waveforms are all similar, and the synthetic waveforms (Langston and Butler, 1976) do not add much insight into determining the

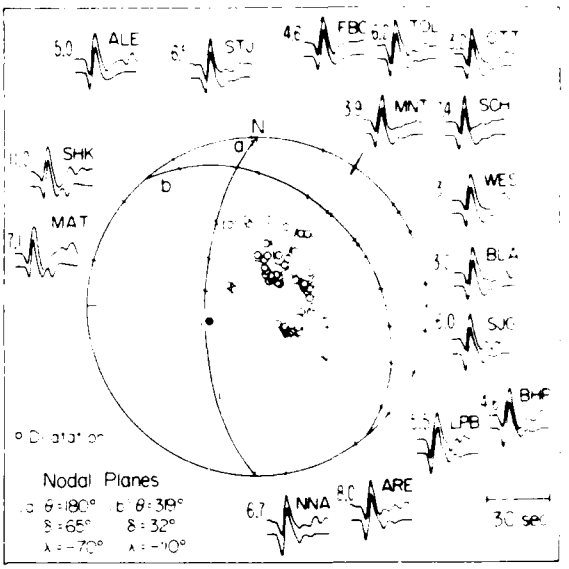

Fig. 11. Teleseismic waveforms from the Oroville earthquake. Note the similarity of the waveforms at all azimuths. Shown on each trace is the moment ($\times 10^{25}$ dyne cm) determined at that station. Note the scatter over a factor of 3 (figure from Langston and Butler, 1976).

strike of the fault. Figure 12 shows the filtered regional data and synthetic waveforms computed from the teleseismic fault-parameter determinations. A comparison of Figs. 12 and 8 shows that the regional data-inversion solution improves the fit of the synthetic waveforms, in particular PAS. This suggests that a logical approach would be to invert some teleseismic data and the regional data simultaneously. Since the inversion technique relies on the cross-correlation of data and a synthetic waveform, the joint inversion is quite tractable.

The higher resolution of the strike-slip events is actually fortuitous. Moderate-size strike slip earthquakes rarely produce usable teleseismic P waves, owing to their inefficiency in radiating energy straight down. On the other hand, strike slip events produce very good regional waveforms. This allows the inclusion of a larger data set in the inversion, and hence the resolution problem is at least partly resolved.

It is reasonable to consider what effect the structural model has on the inversion results. As a

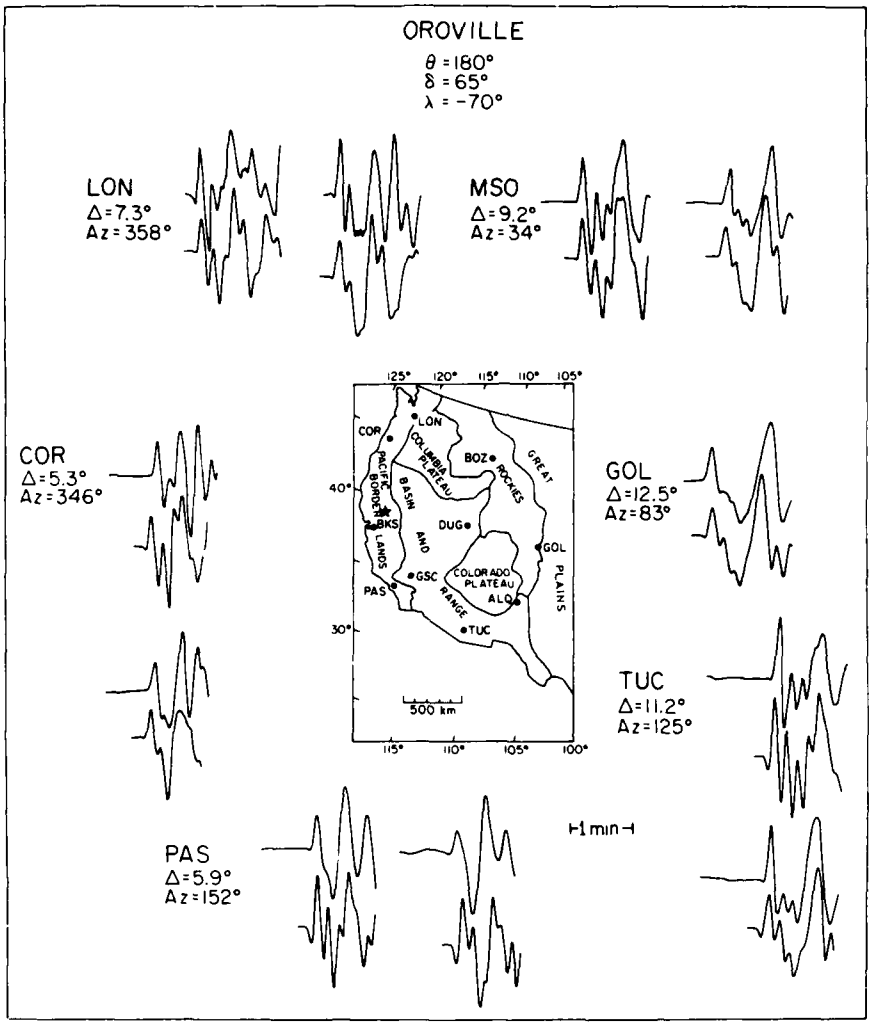

Fig. 12. Filtered P_{nl} waveforms from the Oroville earthquake. The synthetic waveforms were computed with the teleseismic fault-plane solution.

test of the insensitivity of the fault orientation to small changes in crustal parameters the El Golfo earthquake was reinverted with a different structure. The crustal thickness was reduced to 24 km, the source depth was moved to 12 km, and the Pn velocity reduced to 7.8 km s^{-1}. Although the quality of the fit decreases significantly the mechanism returned by the inversion is similar; strike 138°, dip 82°, and rake 181°. The moment increases to 6.9×10^{25} dyne cm.

6. Conclusion

It is possible to extract the source parameters of moderate-size earthquakes from long-period re-

gional body waves. The procedure requires the comparison of the observed with a synthetic waveform; the synthetic waveforms can be generated by a linear combination of the waveforms of the three fundamental faults, shown in Figs. 3 and 4. Although these synthetic waveforms are for a simple model the inversion parameters (fault strike, dip and rake) are fairly insensitive to small changes in crustal thickness, Pn velocity and mean crustal velocity. This allows this single set of Green's functions to be used for most continental earthquakes. The inversion procedure requires only a small data set, and is particularly ideal for strike-slip earthquakes.

Acknowledgements

We would like to thank Gladys Engen and Thorne Lay for reviewing the manuscript. This research was supported by the Advanced Research Projects Agency of the Department of Defense and monitored by the Air Force Office of Scientific Research under Contract F49620-77-C-0022.

References

Burdick, L.J., 1977. Broad-band seismic studies of body waves. Ph.D. Thesis, California Institute of Technology, Pasadena, CA.

Ebel, J.E. Burdick, L.J. and Stewart, G.S., 1978. The source mechanism of the August 7, 1966 El Golfo earthquake. Bull. Seismol. Soc. Am., 68: 1281–1292.

Hart, R.S., Butler, R. and Kanamori, H., 1977. Surface-wave constraints on the August 1, 1975 Oroville earthquakes. Bull. Seismol. Soc. Am., 68: 301–316.

Helmberger, D.V., 1974. Generalized ray theory for shear dislocations. Bull. Seismol. Soc. Am., 64: 45–64.

Helmberger, D.V. and Engen, G.R., 1980. Modeling the long-period body waves from shallow earthquakes at regional distances. Bull. Seismol. Soc. Am., 70: 1699–1714.

Helmberger, D.V. and Malone, S.D., 1975. Modeling local earthquakes as dislocations in a layered half space. J. Geophys. Res., 80: 4881–4888.

Langston, C.A. and Butler, R., 1976. Focal mechanism of the August 1, 1975 Oroville earthquake. Bull. Seismol. Soc. Am., 66: 1111–1120.

Langston, C.A. and Helmberger, D.V., 1975. A procedure for modeling shallow dislocations. Geophys. J., R. Astron. Soc., 42: 117–130.

Liu, H.L. and Kanamori, H., 1980. Determination of source parameters of midplate earthquakes from the waveforms of bodywaves. Bull. Seismol. Soc. Am., 70: 1989–2004.

McKenzie, D., 1972. Active tectonics of the Mediterranean region. Geophys. J., R. Astron. Soc., 30: 109–185.

Ryall, A., Van Wormer, J.D. and Jones, A.J., 1968. Triggering of microearthquakes by earthtides and other features of the Truckee, California earthquake sequence of September, 1966. Bull. Seismol. Soc. Am., 66: 215–248.

Tsai, Y.B. and Aki, K., 1970. Source mechanism of the Truckee, California earthquake of September, 12, 1966. Bull. Seismol. Soc. Am., 60: 1199–1208.

Wallace, T.C. and Helmberger, D.V., 1980. Some useful approximations for modeling P_{nl}. Eos, 61: 1046.

Wallace, T.C. and Helmberger, D.V., 1981. A procedure to account for the effects of upper mantle gradients on P_{nl}. Earthquake Notes, 52: 32.

Wallace, T.C., Helmberger, D.V. and Mellman, G.R., 1981. A technique for the inversion of regional data in source parameter studies. J. Geophys. Res., 86: 1679–1685.

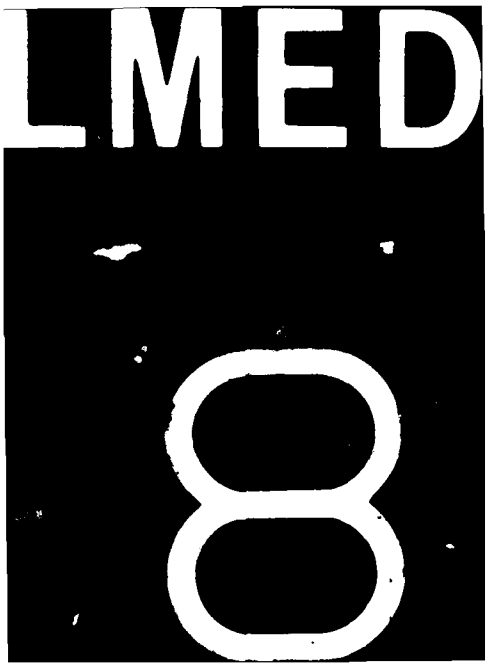
LMED
8